nature photonics

LETTERS

PUBLISHED ONLINE: 17 JANUARY 2010 | DOI: 10.1038/NPHOTON.2009.269

Laser cooling of solids to cryogenic temperatures

Denis V. Seletskiy[1], Seth D. Melgaard[1], Stefano Bigotta[2†], Alberto Di Lieto[2], Mauro Tonelli[2] and Mansoor Sheik-Bahae[1*]

Laser radiation has been used to cool matter ranging from dilute gases to micromechanical oscillators. In Doppler cooling of gases, the translational energy of atoms is lowered through interaction with a laser field[1,2]. Recently, cooling of a high-density gas through collisional redistribution of radiation has been demonstrated[3]. In laser cooling of solids, heat is removed through the annihilation of lattice vibrations in the process of anti-Stokes fluorescence[4–6]. Since its initial observation in 1995, research[7–15] has led to achieving a temperature of 208 K in ytterbium-doped glass[16]. In this Letter, we report laser cooling of ytterbium-doped $LiYF_4$ crystal to a temperature of ~155 K starting from ambient, with a cooling power of 90 mW. This is achieved by making use of the Stark manifold resonance in a crystalline host, and demonstrates the lowest temperature achieved to date without the use of cryogens or mechanical refrigeration. Optical refrigeration has entered the cryogenic regime, surpassing the performance of multi-stage Peltier coolers.

The process of optical refrigeration in solids is based on anti-Stokes fluorescence (Fig. 1). Laser light of frequency ν tuned below the mean emission frequency ($\nu < \bar{\nu}_f$) produces a non-equilibrium electron distribution in the manifolds of the initial and final states. The interaction of these excitations with the lattice leads to phonon absorption followed by blueshifted fluorescence. Heat and entropy are carried away by the fluorescence photons, resulting in net cooling of the material[17].

Research in the field of solid-state laser cooling has primarily focused on rare-earth-doped materials. Semiconductors have also been investigated because of their potential to achieve lower temperatures (<20 K) and their higher cooling capacity[6,18–20]. However, research in this area is still at an early stage[6]. Optical refrigeration is distinguished from opto-mechanical cooling of microscale objects, in which Brownian motion along only one dimension is reduced by use of radiation pressure. Recently, micromechanical resonators have been cooled along the cavity axis, leading to very low 'effective' temperatures[21].

The two essential conditions for achieving net cooling in solids are (i) high external quantum efficiency (EQE) transitions and (ii) extremely high-purity materials with low parasitic loss[6]. The EQE (η_{ext}) describes the probability that an excited atom (ion) will emit a photon that exits the material. It is given by the ratio $\eta_e W_{rad}/(\eta_e W_{rad} + W_{nr})$, where W_{rad} and W_{nr} are the radiative and non-radiative recombination rates, respectively. The extraction efficiency η_e represents the fraction of photons that are not lost to total internal reflection and reabsorption and escape the material. A high EQE can be achieved with rare-earth ions in hosts such as fluoride or chloride glasses and crystals that have low phonon energy. The parasitic loss can be reduced in laser cooling materials by using high-purity starting components in an ultra-clean environment. These requirements are captured in an expression for the cooling efficiency, defined as the ratio of heat lift power to the absorbed laser power[6]:

$$\eta_c(\nu, T) = \eta_{ext}\left[\frac{1}{1+\alpha_b/\alpha(\nu,T)}\right]\frac{\bar{\nu}_f(T)}{\nu} - 1 \qquad (1)$$

where ν is the laser frequency, T the temperature of the solid, $\bar{\nu}_f(T)$ is the escaped mean luminescence frequency, including effects of reabsorption, and $\alpha(\nu, T)$ is the resonant absorption coefficient of the active ion. Parasitic losses are denoted by a frequency- and temperature-independent background absorption coefficient α_b. Background absorption occurs mainly because unwanted contaminants such as transition metal impurities are present during synthesis[22]. The bracketed term in equation (1) defines the absorption efficiency, $\eta_{abs} = (1 + \alpha_b/\alpha(\nu,T))^{-1}$. The product $\eta_{ext}\eta_{abs}$ is therefore interpreted as the fraction of absorbed photons that escape as fluorescence

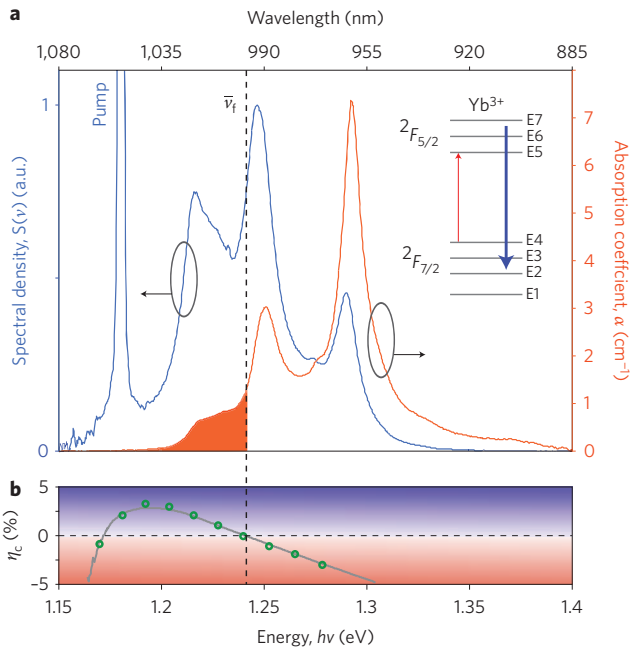

Figure 1 | Optical absorption, emission and cooling efficiency spectra of 5% doped Yb^{3+} ion in a YLF crystal. a, Absorption (red) and fluorescence emission (blue) spectra, for a pump at $\lambda = 1{,}055$ nm polarized along the *c*-axis. The cooling tail corresponding to the absorption spectrum for photon energies below mean fluorescence energy ($h\bar{\nu}_f$) is shaded in red. Inset: energy levels of the ground-state $^2F_{7/2}$ and the excited state $^2F_{5/2}$ containing seven Stark manifolds (E1–E7). **b**, Experimental (open circles) and model fit (line) to cooling efficiency at 300 K.

[1]University of New Mexico, Physics and Astronomy Department, 800 Yale Boulevard NE, Albuquerque, New Mexico 87131, USA, [2]NEST-CNR-INFM, Dipartimento di Fisica, Università di Pisa, Largo B. Pontecorvo 3, 56127 Pisa, Italy. †Present address: French-German Research Institute of Saint-Louis ISL, 5, rue du Général Cassagnou, BP 70034, 68301 Saint-Louis Cedex, France. *e-mail: msb@unm.edu

© 2010 Macmillan Publishers Limited. All rights reserved.

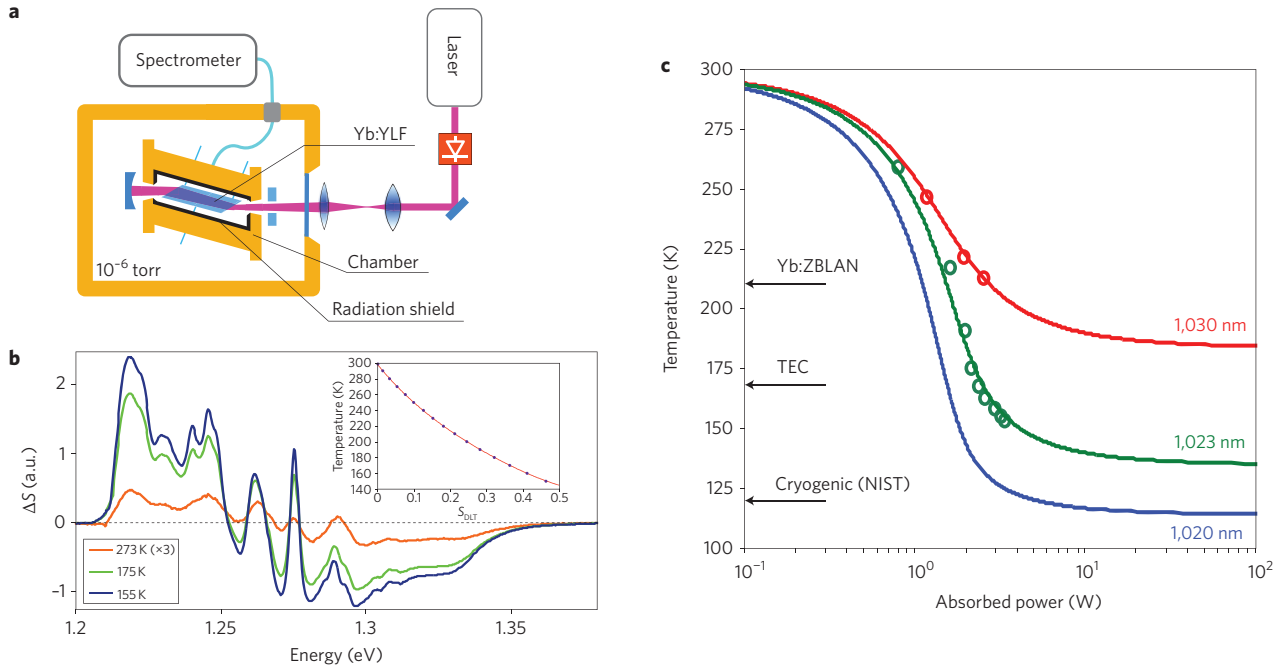

Figure 2 | Experimental arrangement and cooling data for Yb:YLF. a, Schematic of the cavity-enhanced laser cooling set-up. **b**, Differential luminescence spectra ΔS (equation (3)) at various temperatures referenced to $T_0 = 300$ K. The inset shows the calibration curve S_{DLT}, obtained as described in the Methods. **c**, Temperature data (circles) and model fits (lines) obtained using equation (2) versus absorbed power at different wavelengths. A temperature of ~115 K is predicted at the peak of E4–E5 excitation (1,020 nm). The arrows indicate (i) the previous cooling record in ytterbium-doped glass, (ii) the lowest temperature accessible by standard thermoelectric coolers and (iii) NIST-defined cryogenic temperature.

photons. In equation (1), $\eta_c > 0$ implies net cooling. Practical considerations limit the pump detuning to $h\bar{\nu}_f - h\nu \approx k_B T$, leading to the net cooling condition, $\eta_{ext}\eta_{abs} > 1 - k_B T/h\bar{\nu}_f$. For Yb^{3+} systems at 100 K, for example, we require $\eta_{ext}\eta_{abs} > 0.99$. The absorption efficiency (η_{abs}) depends on the ratio α_b/α and can be improved by either reducing impurities (lowering α_b) or increasing the doping concentration (increasing α). The results reported here are made possible by taking advantage of the latter. Note that the cooling efficiency of equation (1) assumes that the fluorescence photons completely escape the system. Capturing and recycling this photon 'waste' with photovoltaic power converters will push the cooling efficiency toward the Carnot limit[23].

In 1995, experiments at Los Alamos National Lab attained 0.3 K cooling in Yb^{3+}-doped fluorozirconate glass Yb:ZBLAN[5]. Improvements led to an absolute temperature of 208 K starting from room temperature, with a corresponding heat lift of 30 mW (ref. 16). Fluorozirconate glasses can be synthesized with high purity, but high dopant concentrations are not stochiometrically allowed and the material is slightly hygroscopic. Furthermore, the large inhomogeneous broadening in a disordered host leads to diminishing resonant absorption at low temperatures. High-purity samples are therefore essential for maintaining a sufficiently high η_{abs}. Fluoride crystals, on the other hand, are not hygroscopic and have a low phonon energy. They have negligible thermal dissipation for radiative transitions and allow for higher doping concentrations, with strong crystal field splitting leading to sharp Stark manifolds with much higher resonant absorption. This relaxes the stringent purity required for glass without sacrificing absorption efficiency.

We investigated high-purity 5% ytterbium-doped YLF crystal in the E//c orientation to increase the pump absorption. The samples were grown in a home-made Czochralski furnace[24]. Absorption and emission spectra were obtained in the temperature range 80–300 K; Fig. 1a shows data at 300 K. We used a broadly tunable Ti:sapphire laser to perform a fractional heating/cooling experiment[6,18] as a function of pump photon energy. This yields the cooling efficiency shown in Fig. 1b. Analysis of this data using equation (1) indicates $\eta_{ext} = 0.995$ and $\alpha_b = 4.2 \times 10^{-4}\,cm^{-1}$. The deduced background absorption coefficient agrees with an earlier, independent measurement[25]. Both of these values are known to be negligibly dependent on temperature and are taken as constant.

The laser cooling set-up is outlined in Fig. 2a (details are presented elsewhere[25]). A thin-disk diode-pumped Yb:YAG excitation laser (35 W at 1,030 nm) was tuned to 1,023 nm to excite close to the E4–E5 transition[26] with a power of 9 W. The laser was mode-matched via a lens pair to a multi-pass cavity placed inside a high-vacuum chamber. The laser and cavity were optically isolated. A Brewster-cut sample measuring $10 \times 3 \times 3\,mm^3$ was positioned inside the cavity defined by highly reflective mirrors with a small entrance hole in the input mirror[27]. The pump beam, with a diameter of 300 μm, made an estimated eight round-trip passes through the sample. Sample temperature was monitored using non-contact differential luminescence thermometry (DLT), which deduces the real-time temperature from variations of fluorescence lineshapes, with a sensitivity of 0.1° (ref. 28) and an accuracy of ~1° across the full temperature range (Fig. 2b).

Careful attention was paid to thermal load management on the sample. The main heat load is black-body radiation, so the crystal was closely surrounded by a copper chamber coated inside with a low-thermal-emissivity material. The coating was also highly absorbing at the fluorescence wavelengths. We estimate that this enclosure reduced the radiative load by a factor of six. The sample was mechanically supported by seven optical fibres protruding from the chamber walls, minimizing the conductive heat load. Cooling experiments were performed at two different excitation wavelengths while adjusting the absorbed power (Fig. 2c). To model the power scaling dependence, we performed spectroscopic analysis of the Yb:YLF emission for the E//c orientation at varying temperatures. Calibrated absorption curves were extracted by reciprocity analysis[29]. We performed model fits on the data

© 2010 Macmillan Publishers Limited. All rights reserved.

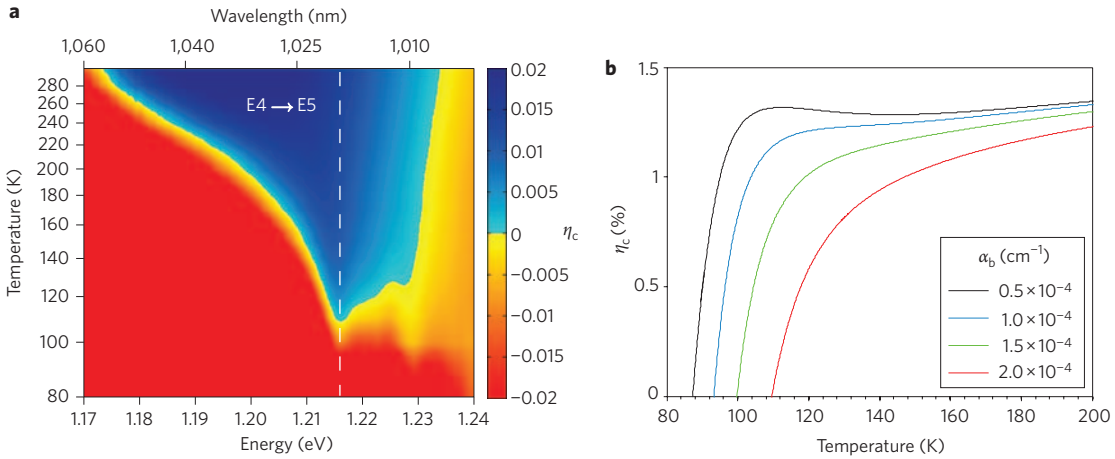

Figure 3 | Parametric representation of the cooling efficiency in 5% doped Yb:YLF crystal. a, Cooling efficiency surface plot versus photon energy and lattice temperature for $\eta_{ext} = 0.995$ and $\alpha_b = 4.2 \times 10^{-4}$ cm^{-1}. The peak of the E4–E5 transition corresponding to $\lambda = 1{,}020$ nm is identified with the dashed line. **b**, Cooling efficiency as a function of temperature at 1,020 nm for various background absorption coefficients assuming $\eta_{ext} = 0.995$.

using measured $\eta_{abs}(\nu,T)$, η_{ext}, and assuming black-body radiation was the dominant heat load (Stefan–Boltzmann law):

$$\eta_c(\nu, T)P_{abs}(\nu, T) = \kappa(T_c^4 - T^4) \qquad (2)$$

where T_c is the chamber temperature and κ is the radiation load constant, which depends on the geometry and joint thermal emissivities of the chamber and sample[27].

At the maximum available absorbed power of 3.5 W at 1,023 nm, the sample cools to 155 ± 1 K absolute temperature. We estimate a heat lift of nearly 90 mW based on the known resonant absorption values. Figure 2b shows this temperature is near the minimum attainable temperature of 140 ± 1 K, indicating adequate performance of the cavity and appropriate heat load management. The minimum temperature is constrained by population depletion of the ground-state manifold of ytterbium, leading to diminishing resonant absorption and cooling efficiency. The wavelength range of the excitation is limited by the pump laser, so we used the model to predict cooling performance when pumping directly at the E4–E5 transition of 1,020 nm (Fig. 2c). Direct wavelength scaling shows that NIST-defined cryogenic operation (<123 K) will be attained. This optical refrigerator surpasses multi-stage thermoelectric cooler (TEC) performance in both absolute temperature and useful heat lift[30]. Optical refrigeration is the only known means of reaching cryogenic temperatures with an all solid-state system.

Our model uses measured values of $\eta_{abs}(\nu,T)$ and η_{ext} that let us plot cooling efficiency as a function of both frequency and temperature (Fig. 3a). The E4–E5 transition produces maximum cooling efficiency, where a minimum temperature of 110 K is predicted for our sample parameters. Even lower temperatures and higher cooling efficiencies are expected upon enhancement of η_{abs} by higher purity and/or ytterbium concentration. For a fixed doping density, an eightfold improvement in sample purity will result in achievable temperatures near nitrogen liquefaction (Fig. 3b). A cooling efficiency of 1.25% would be possible at 100 K, which makes the technology practical for many applications.

In summary, this work demonstrates a new milestone in the field of laser cooling of solids. By making use of the sharp Stark resonance of ytterbium ions doped into a crystalline solid, an absolute temperature of 155 ± 1 K accompanied by 90 mW of heat lift have been achieved with a single-stage refrigerator. This surpasses the performance of currently available Peltier coolers. Analysis shows that a minimum temperature of 110 K is possible for existing Yb:YLF crystals when excited directly at the E4–E5 transition with sufficient laser power. Modest improvements to material purity should allow liquid nitrogen temperature to be reached. Laser cooling of solids has evolved from a laboratory curiosity in 1995 to the only tenable approach for attaining cryogenic temperatures using all solid-state components.

Methods

Differential luminescence thermometry (DLT) was used as a sensitive, non-contact measurement of temperature[27], because thermal (bolometric) cameras become ineffective at $T < 250$ K. Temperature-dependent emission spectra $S(\lambda,T)$ were obtained in real time and referenced to a corresponding spectrum at a starting temperature T_0. The normalized differential spectrum is defined as

$$\Delta S(\lambda, T, T_0) = \frac{S(\lambda, T)}{\int S(\lambda, T)\mathrm{d}\lambda} - \frac{S(\lambda, T_0)}{\int S(\lambda, T_0)\mathrm{d}\lambda} \qquad (3)$$

Normalization to an integrated area or spectral peak was performed to eliminate the effects of input power fluctuations. The saturation of pump absorption could be ignored, as we estimate it to be at least an order of magnitude below saturation intensity[24]. Measured differential spectra for Yb:YLF are shown in Fig. 2b for $T_0 = 300$ K. The sign of the temperature change ($\Delta T = T - T_0$) is inferred from the spectral shape. The scalar DLT signal is the absolute area of the differential spectrum: $S_{DLT}(T, T_0) = \int_{\lambda_1}^{\lambda_2} \mathrm{d}\lambda |\Delta S(\lambda, T, T_0)|$, where the limits of integration bracket the spectral emission of the Yb:YLF, eliminating possible contributions from spurious laser line scatter. This signal was converted to an absolute temperature through a separate calibration process. The sample was mounted in an optical cryostat in which unpolarized fluorescence spectra were recorded as a function of temperature. The geometry closely mimics the laser cooling set-up to mitigate the effect of fluorescence reabsorption. Sample fluorescence was collected through a multimode 600-μm core diameter fibre that was used for both calibration and cooling experiments. The resultant calibration curve, together with a polynomial fit, is shown in the inset of Fig. 2b.

DLT is intrinsically a local probe of temperature. In our experiments, however, we detected the bulk (spatially uniform) temperature of the sample due to (i) a multipass pumping geometry that illuminates nearly the entire sample volume and (ii) high thermal conductivity in the YLF crystal, which diminishes any remaining thermal gradients resulting from non-uniform pumping within less than a second (which is more than an order of magnitude shorter than the thermal response time of the experiment[16]). Temperature homogeneity was further verified by imaging the entire sample with a thermal camera at a small temperature drop (~10°).

Received 4 October 2009; accepted 2 December 2009; published online 17 January 2010

References

1. Hänsch, T. W. & Schawlow, A. L. Cooling of gases by laser radiation. *Opt. Commun.* **13,** 68–69 (1975).
2. Chu, S., Cohen-Tannoudji, C. & Philips, W. D. For development of methods to cool and trap atoms with laser light. *Nobel Prize in Physics* http://nobelprize.org (1997).

© 2010 Macmillan Publishers Limited. All rights reserved.

3. Vogl, U. & Weitz, M. Laser cooling by collisional redistribution of radiation. *Nature* **461,** 70–74 (2009).
4. Pringsheim, P. Zwei bemerkungen über den unterschied von lumineszenz- und temperaturstrahlung. *Z. Phys.* **57,** 739–746 (1929).
5. Epstein, R. I., Buchwald, M., Edwards, B., Gosnell, T. & Mungan, C. Observation of laser induced fluorescent cooling of a solid. *Nature* **377,** 500–503 (1995).
6. Sheik-Bahae, M. & Epstein, R. I. Optical refrigeration. *Nature Photon.* **12,** 693–699 (2007).
7. Mungan, C. E., Buchwald, M. I., Edwards, B. C., Epstein, R. I. & Gosnell, T. R. Laser cooling of a solid by 16 K starting from room temperature. *Phys. Rev. Lett.* **78,** 1030–1033 (1997).
8. Bowman, S. R. & Mungan, C. E. New materials for optical cooling. *Appl. Phys. B* **71,** 807–811 (2000).
9. Hoyt, C. W., Sheik-Bahae, M., Epstein, R. I., Edwards, B. C. & Anderson, J. E. Observation of anti-Stokes fluorescent cooling in thulium-doped glass. *Phys. Rev. Lett.* **85,** 3600–3603 (2000).
10. Mendioroz, A. *et al.* Anti-Stokes laser cooling in Yb^{3+}-doped KPb_2Cl_5 crystal. *Opt. Lett.* **27,** 1525–1527 (2002).
11. Fernandez, J., Garcia-Adeva, A. J. & Balda, R. Anti-Stokes laser cooling in bulk erbium-doped materials. *Phys. Rev. Lett.* **97,** 033001 (2006).
12. Bigotta, S. *et al.* Spectroscopic and laser cooling results on Yb^{3+}-doped BaY_2F_8 single crystal. *J. Appl. Phys.* **100,** 013109 (2006).
13. Bigotta, S. *et al.* Laser cooling of solids: new results with single fluoride crystals. *Nuovo Cimento B Serie* **122,** 685694 (2007).
14. Patterson, W. *et al.* Anti-Stokes luminescence cooling of Tm^{3+} doped BaY_2F_8. *Opt. Express* **16,** 1704–1710 (2008).
15. Condon, N. J., Bowman, S. R., O'Connor, S. P., Quimby, R. S. & Mungan, C. E. Optical cooling in Er^{3+}:KPb_2Cl_5. *Opt. Express* **17,** 5466–5472 (2009).
16. Thiede, J., Distel, J., Greenfield, S. R. & Epstein, R. I. Cooling to 208 K by optical refrigeration. *Appl. Phys. Lett.* **86,** 154107 (2005).
17. Epstein, R. I. & Sheik-Bahae, M. *Optical Refrigeration* (Wiley-VCH, 2009).
18. Gauck, H., Gfroerer, T. H., Renn, M. J., Cornell, E. A. & Bertness, K. A. External radiative quantum efficiency of 96% from a GaAs/GaInP heterostructure. *Appl. Phys. A* **64,** 143–147 (1997).
19. Sheik-Bahae, M. & Epstein, R. I. Can laser light cool semiconductors? *Phys. Rev. Lett.* **92,** 247403 (2004).
20. Finkeissen, E., Potemski, M., Wyder, P., Vina, L. & Weimann, G. Cooling of a semiconductor by luminescence up-conversion. *Appl. Phys. Lett.* **75,** 1258–1260 (1999).
21. Höhberger-Metzger, C. & Karrai, K. Cavity cooling of a microlever. *Nature* **432,** 1002–1005 (2004).
22. Hehlen, M. P., Epstein, R. I. & Inoue, H. Model of laser cooling in the Yb^{3+}-doped fluorozirconate glass ZBLAN. *Phys. Rev. B* **75,** 144302 (2007).
23. Sheik-Bahae, M. & Epstein, R. I. Laser cooling of solids. *Laser Photon. Rev.* **3,** 67–84 (2009).
24. Coluccelli, N. *et al.* Diode pumped passively mode-locked Yb:YLF laser. *Opt. Express* **16,** 2922–2927 (2008).
25. Seletskiy, D. V. *et al.* Cooling of Yb:YLF using cavity enhanced resonant absorption. *Proc. SPIE* **6907,** 6907B (2008).
26. Sugiyama, A., Katsurayama, M., Anzai, Y. & Tsuboi, T. Spectroscopic properties of Yb doped YLF grown by a vertical Bridgman method. *J. Alloy Compound* **408–412,** 780–783 (2006).
27. Hoyt, C. W. *et al.* Advances in laser cooling of thulium-doped glass. *J. Opt. Soc. Am. B* **20,** 1066–1074 (2003).
28. Imangholi, B. *et al.* Differential luminescence thermometry in semiconductor laser cooling. *Proc. SPIE* **6115,** 61151C (2006).
29. McCumber, D. E. Einstein relations connecting broadband emission and absorption spectra. *Phys. Rev.* **136,** A954–A957 (1964).
30. Mills, G. & Mord, A. Performance modeling of optical refrigerators. *Cryogenics* **46,** 176–182 (2005).

Acknowledgements

This work has been supported by the Air Force Office of Scientific Research (MURI program), grant FA 9550-04-1-0356. The authors thank M.P. Hasselbeck and R.I. Epstein for helpful discussions and M.P. Hasselbeck for proofreading the manuscript. The authors would also like to acknowledge the skill and competence of I. Grassini in preparing the sample.

Author contributions

D.V.S. and M.S.B. designed and implemented the experiments. D.V.S. and S.D.M. performed the experiments, designed radiation shielding and carried out calibrations. S.B., A.D.L. and M.T. grew and prepared the high-purity Yb:YLF crystals and provided supporting spectroscopic data. All authors contributed to the final manuscript.

Additional information

The authors declare no competing financial interests. Reprints and permission information is available online at http://npg.nature.com/reprintsandpermissions/. Correspondence and requests for materials should be addressed to M.S.B.

© 2010 Macmillan Publishers Limited. All rights reserved.